Influence of SiO$_2$ and CaO additions on the microstructure and magnetic properties of sintered Sr-hexaferrite

J. Töpfer[a,b,*], S. Schwarzer[b,1], S. Senz[c], D. Hesse[c]

[a] *Fachhochschule Jena, FB Werkstofftechnik, Carl Zeiss Promenade 2, 07745 Jena, Germany*
[b] *Hermsdorfer Institut für Technische Keramik e.V., M.-Faraday-Str. 1, 07629 Hermsdorf, Germany*
[c] *Max-Planck-Institut für Mikrostrukturphysik, Weinberg 2, 06120 Halle, Germany*

Abstract

The effect of simultaneous addition of CaO and SiO$_2$ on the microstructure and magnetic properties of sintered SrO-excess Sr-hexaferrites was studied. Both additives markedly affect the grain growth behavior and the magnetic properties. CaO-additions promote densification, which results in increased remanence, but due to simultaneuous grain growth the coercivity drops to <100 kA/m. SiO$_2$ additions are known to suppress grain growth. Simultaneous addition of CaO and SiO$_2$ is shown to be very beneficial in tailoring a dense microstructure with relatively small grains. The ratio of CaO/SiO$_2$ was found to be optimum at about 1, and magnets with a remanence of 430 mT and a coercivity of 300 kA/m were obtained. Transmission electron microscopy (TEM) studies and investigations by energy-dispersive analysis of X-rays (EDX) in the scanning TEM (STEM) mode show that both CaO and SiO$_2$ are concentrated at grain boundaries and grain junctions forming an amorphous secondary phase.
© 2004 Elsevier Ltd. All rights reserved.

Keywords: Ferrites; Hard magnets; Grain size; Grain boundaries; S$_5$Fe$_{12}$O$_{19}$

1. Introduction

Hard ferrites of the Ba- or Sr-hexaferrite system are the major permanent magnetic material. These magnets are manufactured on large scale worldwide (300.000 and 50.000 t per year in Europe in 1994[1]). Hard ferrites have been introduced as new technically important magnetic materials in the 1950.[2] Recently, Kools et al.[3] have reviewed the status of this mature family of ceramic materials. Nevertheless, the improvement of ferrite materials with respect to specific material parameters or application fields is still a vital field of research.

One crucial issue is the development of ferrite grades with large remanence and energy product. Standard hard ferrites are manufactured as anisotropic ferrites, i.e. the ferrite particles are oriented in a magnetic field during molding. A large remanence $B_R = J_S \alpha \rho$ requires a high density ρ and anisotropy factor α of the sintered microstructure. If both quantities approach 100% the remanence becomes equal to the saturation polarization J_S. With a saturation magnetization of 74.3 emu/g at room temperature for SrFe$_{12}$O$_{19}$[4] B_R of a sintered magnet is 0.476 T at maximum. In practice, the remanence of a typical high-remanence ferrite is B_R = 400–420 mT. This is due to (i) the composition being not that of a stochiometric ferrite SrO·6Fe$_2$O$_3$ (magnets are prepared with an excess of SrO) and (ii) the particle orientation being non-ideal and some residual porosity remaining. For high-remanence materials it is essential to create a dense, anisotropic microstructure by firing at high temperature. On the other hand, grain growth is detrimental with respect to the coercivity because of the formation of multi-domain particles. A large coercivity requires small grains with a size

* Corresponding author. Tel.: +49 3641 20 5450; fax: +49 3641 20 5451.
 E-mail address: joerg.toepfer@fh-jena.de (J. Töpfer).
[1] Present address: Magnetfabrik Schramberg, M.-Planck-Str. 15, 78713 Schramberg-Sulgen, Germany.

smaller than the critical size for single domain particles of about 1 μm.[5] To produce magnets with large remanence and coercivity, it is essential to precisely tailor the ceramic process which in turn controls the complex interplay between a dense microstructure and grain growth. Ferrite powder particles should have dimensions below 1 μm to allow some unavoidable grain growth during sintering and to limit the grain size in the sintered magnets to a few microns. Taguchi[6] and Schwarzer et al.[7] reported on sub-micron powders prepared by improved calcination and milling procedures which allow the preparation of high-performance magnets with large remanence ($B_R = 0.44$ T). Substitution of La and Co for Sr and Fe has emerged as a different approach to increase the ferrite performance, high-remanence magnets with $B_R = 0.45$ T and $H_{CI} > 300$ kA/m have been introduced.[3,8]

The formation of the desired dense microstructure with small oriented grains is controlled by the addition of sintering additives. Several systems have been proposed by Arendt.[9] SiO_2 was introduced as grain growth inhibitor in hexaferrites.[10] The mechanism of the action of SiO_2 in ferrites was studied by Haberey and Kools.[11,12] The sintering behavior and mechanism of grain boundary motion hindrance was studied in detail by Kools[13,14] and a new mechanism of reaction induced grain growth impediment (RIGGI) has been proposed. Simultaneous addition of 0.45% CaO and 0–0.6% SiO_2 as another option to suppress grain growth has been investigated; a large remanence and a coercivity of 250 kA/m were obtained.[15] Moreover, there are some indications that the size of the additives might also play a crucial role in determining their effectiveness for microstructure control. Positive effects of fine-grained silica[16] and the uniform incorporation of Ca and Si utilizing a sol–gel route[17] were demonstrated.

In this paper we report on microstructural control of the magnetic properties by simultaneously adding CaO and SiO_2 in a concentration range from 0 to 1 wt.%. We address the following issues: (i) determination of the optimum additive concentrations and (ii) role of additives in microstructure formation. Using both additives we prepared anisotropic dense Sr-ferrite magnets with a remanence of $B_R = 430$–440 mT and a coercivity $H_{CI} = 250$–300 kA/m.

2. Experimental

2.1. Sample preparation

All ferrite samples were prepared using the standard ceramic process. The raw materials $SrCO_3$ (grade B, Solvay Barium Strontium GmbH, Hannover, Germany) and Fe_2O_3 (EKO Recycling GmbH, Eisenhüttenstadt, Germany) were mixed in a molar ratio SrO:Fe_2O_3 = 1:5.6–5.8 and granulated. The granules (3–10 mm diameter) were calcined at 1300 °C for 0.5 h. The calcined granules were coarse milled in a rotary vibration mill to a specific surface area of $s = 1$–2 m^2/g.

SiO_2 and $CaCO_3$ were added in various concentrations and then the ferrite powders were fine milled in an attrition mill for 24 h (batch size: 2 kg ferrite powder, 20 kg steel balls (3 mm diameter) and 3 l water). This procedure gives a powder with a mean particle size of about 1 μm and a specific surface of 11–12 m^2/g. To study the effect of the additive concentration on the ferrite microstructure samples SF0–SF2 were prepared without any, or with either 0.5 wt.% SiO_2 or CaO addition. In all other samples SiO_2 and CaO were added simultaneously, whereas the total additive concentration (SiO_2 + CaO) of samples SF3–SF7 is 1 wt.% (Table 1). The additives were characterized by their specific surface: SiO_2 (360 m^2/g) and $CaCO_3$ (8 m^2/g). The ferrite slurry was pressed in a magnetic field of 560 kA/m (field parallel to the direction of pressure) into discs of 52 mm in diameter and 4–6 mm in height. The samples were sintered at a peak temperature of 1200–1300 °C.

2.2. Measurements

The particle size of the powders was measured with a Sympatec laser scattering system with a dry dispersion unit (system Rodos). The specific surface of the powders was determined by adsorption of nitrogen in a BET apparatus (Micromeritics). The magnetic properties of the sintered magnets were measured at room temperature with a permagraph (Magnet-Meßtechnik Ballanyi) on polished discs. The ceramic microstructures were analyzed on polished and thermally etched faces of the magnets (parallel to the applied

Table 1
Concentration of additives, S/C ratio (SiO_2/CaO), magnetic properties and density of samples sintered at 1280 °C

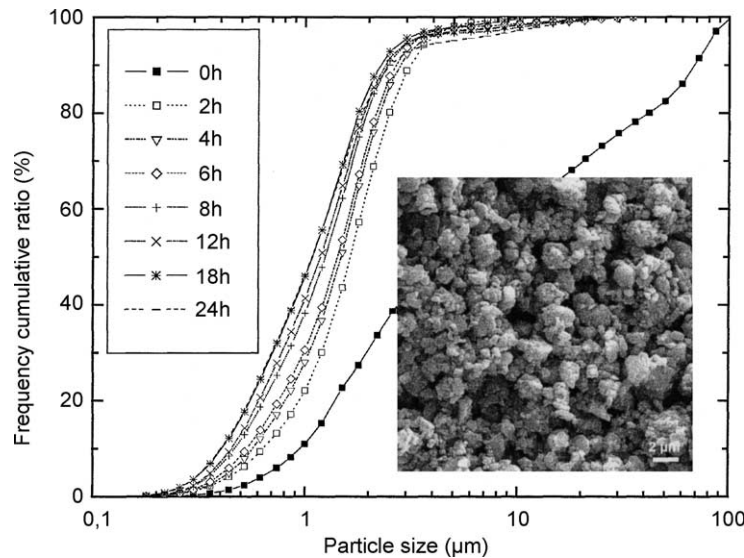| Sample SF	SiO_2 (wt.%)	CaO (wt.%)	S/C ratio	Density (g/cm³)	B_R (mT)	H_{IC} (kA/m)	BH_{max} (kJ/m³)
0	–	–	–	5.03	430	156	–
1	0.50	–	–	4.79	387	296	–
2	–	0.50	–	5.02	433	116	–
3	0.75	0.25	3	4.96	421	284	32.8
4	0.60	0.40	1.5	4.93	415	300	31.6
5	0.50	0.50	1	4.98	424	282	32.6
6	0.40	0.60	0.67	5.05	436	178	26.8
7	0.25	0.75	0.33	4.79	413	118	15.2
8	0.60	0.60	1	4.97	406	289	29.2
9	0.80	0.60	1.33	4.93	398	320	28.7
10	1.00	0.60	1.67	4.94	406	301	28.8

Fig. 1. Particle size distribution of Sr-ferrite powder during attrition milling; inset: SEM micrograph of powder milled for 24 h with $d_{50} = 1$ μm.

pressure and field) by SEM (Zeiss). TEM and EDX analyses were performed with a Philips CM20FEG transmission electron microscope.

The Fe^{2+} concentration was determined by chemical titration after dissolution of the powdered sample in hydrochloric acid in argon. The Fe^{2+} was titrated with a 0.05N Ce^{4+} solution under a flow of argon, with potentiometric detection of the equivalent point. The detection limit of that titration is given by the first drop of Ce^{4+} solution ($V \approx 0.03$ ml), which corresponds to 0.08 wt.% Fe^{2+} for 100 mg of a ferrite sample.

3. Results

The change of the particle size distribution of the Sr-ferrite powder during attrition milling and the morphology of the fine-milled powder with a mean particle size of 1 μm is shown in Fig. 1. The composition of sintered magnets prepared from this powder was controlled by chemical analysis; a ratio $SrO:Fe_2O_3 = 1:5.94$ has been observed.

To optimize the microstructure formation, i.e. to obtain sintered samples with high density and only little grain growth several sintering regimes were tested. One set of sinter experiments was performed at 1250 °C for 45 min. For samples SF3–SF7 a gradual increase in density and grain size with decreasing ratio SiO_2/CaO (S/C) was observed. A serious problem was the appearance of abnormal grain growth. The tendency to form huge grains with size of about 100 μm in a matrix of grains of size of about 2–5 μm also increases with decreasing S/C ratio. The best results were observed with sintering at a peak temperature of 1280 °C for a short period of time after heating (and cooling) the samples with 3 K/min to 1150 °C. Similar results were reported by Besenicar and Drofenik[18] after sintering at 1260 °C for only 3 min they observed an almost dense microstructure (97%) with acceptable magnetic properties.

The microstructure of magnets SF0–SF2 sintered at 1280 °C is shown in Fig. 2. The SEM micrographs were taken perpendicular to the direction of pressure and magnetic field during wet molding; the view is along the basal planes of the platelet shaped ferrite particles. If one takes into
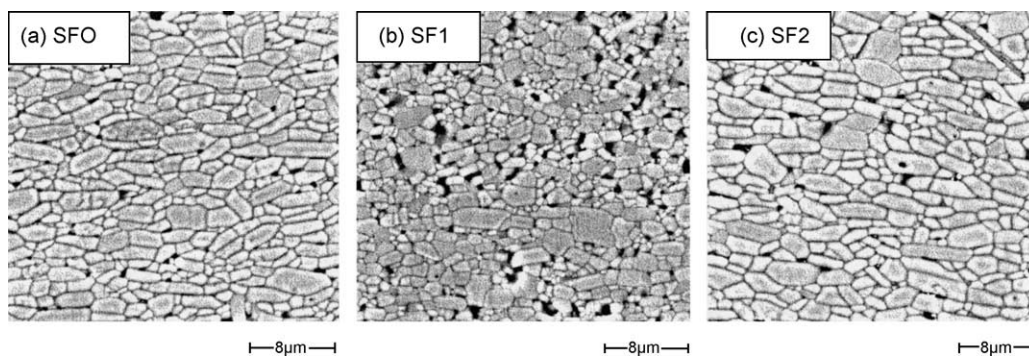

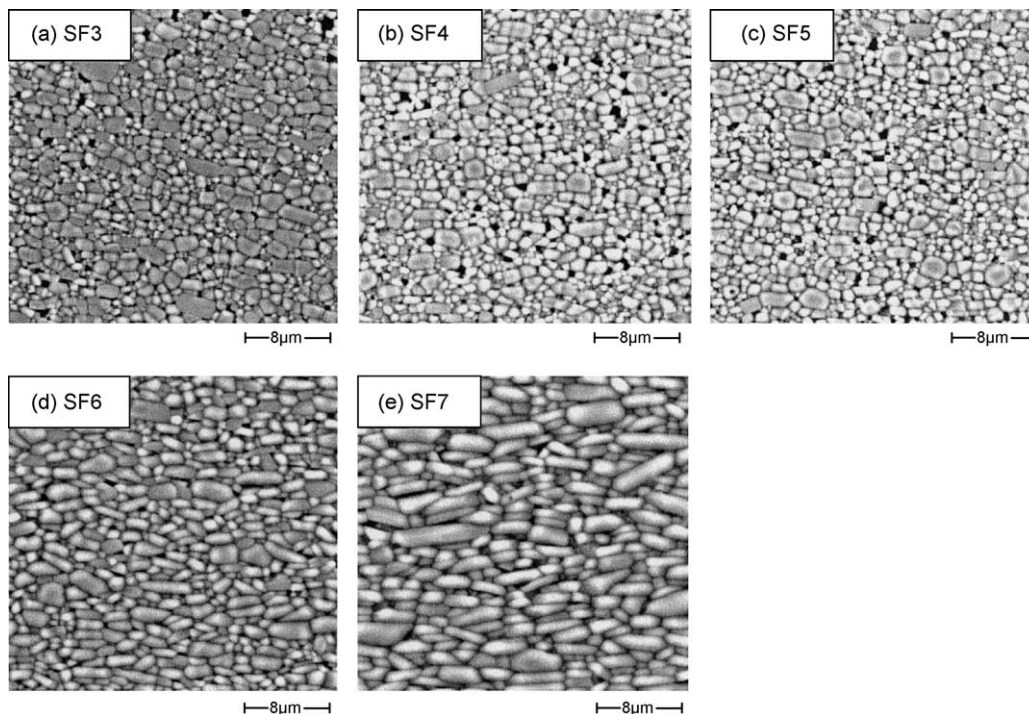Fig. 2. SEM micrographs of sample SF0–SF2 sintered at 1280 °C.

Fig. 3. SEM micrographs of magnets SF3–SF7 sintered at 1280 °C.

account the size of the fine-milled powder of about 1 μm, it is obvious that grain growth predominately occurs perpendicular to the hexagonal *c*-axis. Without additives (SF0) a dense and anisotropic microstructure with platelet-shaped grains of 1–2 μm in height and about 3–5 μm in length is observed. Similar results are obtained for sample SF2 with only CaO addition. Addition of 0.5 wt.% SiO_2 significantly reduced the grain size (SF1, Fig. 2b) as well as the density. The shape of the particles also changes; the particles are less platelet-like with a smaller aspect ratio. This is reflected in the magnetic properties (Table 1). The dense microstructure of magnets SF0 and SF2 is transformed into high remanence, but due to the relatively large platelet-shaped grains the coercivity is low. For magnet SF1 the coercivity is increased to almost 300 kA/m, but B_R is reduced.

The microstructure of samples SF3–SF7 (Fig. 3), i.e. with simultaneous SiO_2 and CaO addition, but various *S/C* ratios, shows significant changes in the size of the grains. Whereas in samples with large *C/S* ratio small grains with 2–3 μm in length are observed, samples with smaller *C/S* ratio show longer grains of up to 5 μm. Grain growth along the hexagonal *c*-axis hardly occurs, whereas perpendicular to this axis the grains grow, i.e. the aspect ratio tends to increase if the *S/C* ratio becomes smaller. The density of the sintered magnets SF3–SF7 (Table 1) slightly increases up to a *S/C* = 0.67, only SF7 with *S/C* = 0.33 has a reduced density of 4.79 g/cm³. The demagnetization curves are shown in Fig. 4, the magnetic parameters are collected in Table 1. The variation of B_R and H_c with the concentration of additives (expressed as *C/S* ratio) is shown in Fig. 5.

The addition of 0.6% CaO (sample SF6) seems very effective for densification, but 0.4% SiO_2 is not sufficient to avoid substantial grain growth and the subsequent decrease of coercivity. A series of magnets (SF8–SF10) with 0.6% CaO and different SiO_2 concentrations was prepared (Table 1). Indeed, the grain size of samples sintered at 1280 °C is reduced compared to sample SF6. Consequently, the coercivity is increased up to around 300 kA/m. On the contrary, with SiO_2 concentrations increasing from 0.6 to 1% (*S/C* ratio from 0.67 to 1.67) the density of the magnets is reduced to below 5 g/cm³ and thus the remanent induction is also reduced. The increased absolute concentration of non-magnetic additive phase contributes to the reduced B_R.
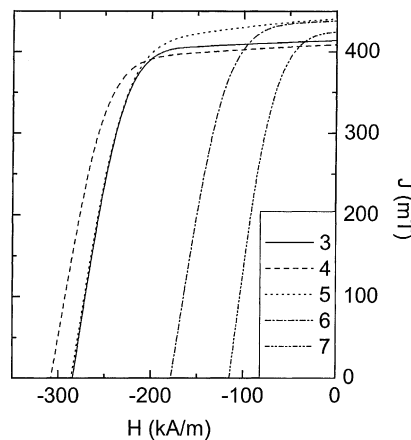

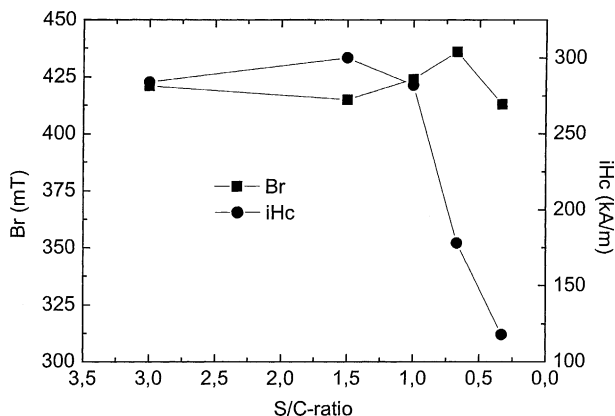Fig. 4. Demagnetization curves of magnets SF3–SF7 sintered at 1280 °C.

Fig. 5. Remanence B_R and coercivity H_{IC} as a function of the S/C ratio (SiO_2/CaO) for magnets SF3–SF7 sintered at 1280 °C.

To check whether the addition of SiO_2 and CaO promotes the formation of Fe^{2+} selected samples were analyzed by chemical titration. SF0 without any additives and SF2 with the addition of 0.5 wt.% CaO have no detectable concentration of Fe^{2+}. Addition of 0.5 wt.% SiO_2 (SF1) gives $0.12 \pm 0.03\%$ Fe^{2+}. For sample SF5 (0.5 wt.% SiO_2 and CaO) no Fe^{2+} was found.

The appearance of the additives in the ceramic microstructure has been studied by STEM and EDX. Fig. 6 shows a three-grain junction between neighboring grains with a dihedral angle of about 60°. The liquid phase continuously wets the grains and a thin grain boundary layer is detected.

Fig. 6. TEM image of a three-grain junction of sample SF5 with 0.5% SiO_2 and 0.5% CaO sintered at 1280 °C.
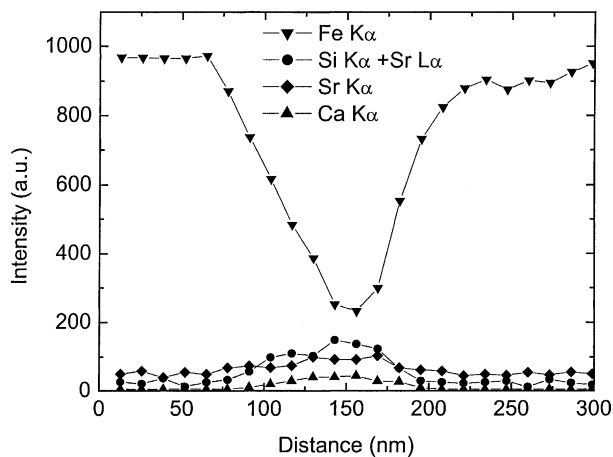

Fig. 7. EDX line scan through a three-grain junction of sample SF5.

The corresponding incoherent dark field transmission image (not shown here) shows that the nature of the solidified grain boundary phase is amorphous. An EDX line scan through one of the triple grain junctions (Fig. 7) shows that the Fe signal is strongly reduced at the center of the junction, whereas Ca is enriched. The detection of Si is more difficult, because of the overlap of the Si-K_α and Sr-L_α signals at about 1.6–2.0 keV. The signal in Fig. 7 contains contributions of both elements and shows increased intensities at the junction; the Sr-K_α signal also shows a slight increase. From that analysis it cannot be concluded whether Si or Sr is enriched at the grain junction. In Fig. 8 a scan is made across another position of the sample. The upper part of Fig. 8 shows the line of the scan crossing a grain junction in the left center of the figure as well as two grain boundaries in the right-hand part of the figure (marked with arrows). The three intergranular areas are also recognized in the scan of the brightness. The iron signal again is strongly reduced at the grain junction and boundaries. To better detect the Si signal, regions of interest (ROI) have been selected (e.g. 1.56–1.8 keV for Si and 1.8–2.0 keV for Sr). Although a complete discrimination between Si and Sr signals is not achieved in this way due to the limited energy resolution of the detector, the sensitivity for the Si signal is considerably higher in the first ROI, and that for the Sr signal in the second. The lower panel of Fig. 8 shows the recorded intensities. Unambiguously Si is enriched at the grain junction and grain boundary phase. The variation of the Ca intensity also clearly signals an increase at the grain junction. For the Sr signal a slight enhancement relative to the grain has been observed which does not allow to interpret whether Sr is a significant part of the grain boundary phase or not.

4. Discussion

The role of SiO_2 as an additive for micro-structural control of hard ferrite magnets has been explained as liquid phase forming agent.[9–11] From very detailed studies, the
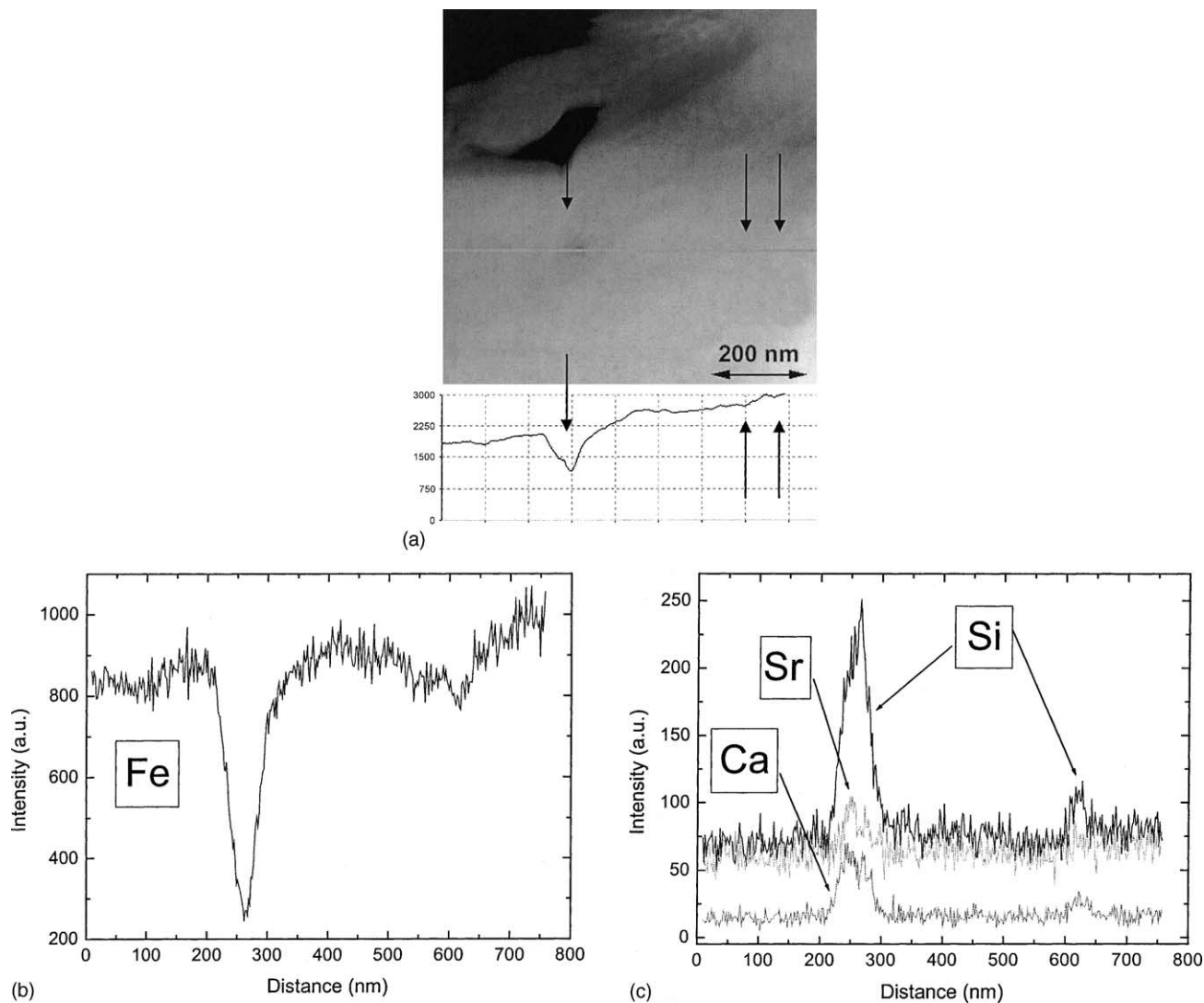
Fig. 8. (a) EDX line scan through sample SF5 crossing one three-grain junction and two grain boundaries (upper panel, marked by arrows) and variation of brightness (lower panel) and (b) and (c) element concentrations as recorded at selected energies.

action of silica has been categorized as being dependent on the ratio SiO_2 additive over SrO-excess concentration.[13,14] Technical hard ferrite compositions have a Fe_2O_3/SrO ratio <6 making the excess SrO a ready candidate for reactions with silica at elevated temperatures. According to the proposed phase diagram $SrO–SiO_2–Fe_2O_3$ at 1250 °C the addition of SiO_2 causes the appearance of liquid or solid minority phases depending on the SiO_2 and SrO-excess concentrations.[14]

If SiO_2 and CaO (or $CaCO_3$) are added simultaneously, both components are expected to react and to form Ca-silicate (CS)-phases at low temperature. The formation of CS-phases has been observed at temperatures as low as 600–800 °C.[19] In the $CaO–SiO_2$ system the first eutectic temperatures appear at 1436 °C,[20] i.e. above the sintering temperature of the ferrite. On the other hand, if Sr-ferrite with excess SrO is sintered above the eutectic temperature of 1210 °C,[21,22] the

liquid phase is expected to react with the calcium silicates formed from CaO and SiO_2 additives. The composition of the liquid phase determines the rate of grain growth of the ferrite particles. During cooling CS-rich phases seem to become solidified as amorphous grain boundary phases as shown by electron microscopy. Another indication for such mechanism is the fact, that only for SF1 a detectable Fe^{2+} concentration has been observed. In agreement with the observations of Kools[14] this is a result of partial incorporation of Si into the ferrite lattice. For SF5 no Fe^{2+} has been found signaling that the reaction of SiO_2 with CaO and not with ferrite is favored.

The magnetic properties of a hexaferrite are determined by its chemistry and microstructure. To obtain high-remanence magnets a dense microstructure with well aligned particles and possibly little non-magnetic secondary phase is necessary. If a large coercivity is desired the particle size should

be in the order of the critical diameter d_c for single domain behavior given by:

$$d_c = \frac{18\sqrt{(AK_1)}}{\mu_0 M_s^2}$$

where K_1 is the magnetocrystalline anisotropy constant, A is the exchange energy constant and M_s is saturation magnetization.[23] For Sr-ferrite $d_c \approx 1\,\mu m$.[5] The coercivity according to the Stoner–Wohlfahrt situation of non-interacting single-domain particles with the anisotropy provided by magneto-crystalline anisotropy is:

$$H_{IC} = 0.48 \left(\frac{2K_1}{\mu_0 M_s} - NM_s \right)$$

where N is the demagnetizing factor.[23] To obtain a high coercivity the material should possess a large anisotropy field. If the grains are platelet-shaped with large aspect ratio the demagnetizing field becomes large and the coercivity is reduced. This makes the grain shape another important factor influencing the coercivity.

The different microstructures of SF0 and SF1 (Fig. 2) confirm that SiO_2 addition is effective for the suppression of grain growth and enhancement of coercivity, but a decreased density causes lowered remanence. Therefore, simultaneous use of SiO_2 and CaO is appropriate to tailor the grain growth inhibition and to promote densification. Inspection of the microstructures of samples SF3–SF7 shows that if the concentration of silica becomes smaller (simultaneously the S/C ratio becomes smaller) the grains progressively start to grow and the aspect ratio increases. If a certain threshold in grain size and grain length (aspect ratio) is reached the coercivity drops to below 250 kA/m. On the other hand, to promote densification and enhance B_R the addition of some CaO is required. The density increases from 4.96 to 5.05 g/cm^3 if the S/C ratio decreases from 3 to 0.67 (Fig. 5). Simultaneously, the remanence is increased up to 436 mT except for sample SF7 with $S/C = 0.33$ where due to the low SiO_2 content grain growth seems to become predominating and densification is incomplete. A S/C ratio of about 1 seems to be optimum for a dense microstructure without significant particle growth. For magnet SF5 with 0.5% SiO_2 and 0.5% CaO high remanence and coercivity were observed.

5. Conclusions

The simultaneous addition of SiO_2 and CaO is well suited to promote the densification of hard ferrite magnets without allowing too much grain growth. For a total additive concentration of 1 wt.% the ratio SiO_2/CaO (S/C) determines the formation of the ceramic microstructure and hence the magnetic properties. For $S/C \geq 1$ a dense microstructure without significant grain growth is observed, whereas for $S/C \leq 1$ grain growth sets in leading to a deterioration of the coercivity. The additives form a Ca-silicate rich amorphous phase at multiple-grain junctions and grain boundaries.

References

1. Hart, W., The global magnetic materials market—past, present and future. In *Proceedings of the Conference "Iron Oxides for Hard/Soft Ferrites, Gorham-Intertec, Pittsburgh*, 1996.
2. Went, J. J., Rathenau, G. W., Gorter, E. W. and van Oosterhout, G. W., Ferroxdure—eine Gruppe neuer Werkstoffe für Dauermagnete. *Philips Techn. Rundschau.*, 1952, **13**, 361–376.
3. Kools, F., Morel, A., Grössinger, R., Le Breton, J. M. and Tenaud, P., LaCo-substituted ferrite magnets, a new class of high-grade ceramic magnets; intrinsic and microstructural aspects. *J. Magn. Magn. Mater.*, 2002, **242–245**, 1270–1276.
4. Shirk, B. T. and Bussem, W. R., Temperature dependence of M_s and K_1 of $BaFe_{12}O_{19}$ and $SrFe_{12}O_{19}$ single crystals. *J. Appl. Phys.*, 1969, **10**, 1294–1296.
5. Smit, J. and Wijn, H. P. J., *Ferrites*. Centrex Verlag, Eindhoven, 1962.
6. Taguchi, H., Recent improvements of ferrite magnets. *J. Phys. IV France*, 1997, **7**(C1), 299–302.
7. Schwarzer, S., Töpfer, J. and Kätzel, D., Preparation of high-remanence $SrFe_{12}O_{19}$-Hexaferrites. *Ceram. Forum Int./Ber. DKG*, 2003, **80**, E39–E44.
8. Taguchi, T., Minachi, Y., Masuzawa, K. and Nishio, H., High performance SrLaCo-ferrite magnets with M-structure. In *Proceedings of the Eight International Conference on Ferrites (ICF8), Kyoto, Japan*, 2000, pp. 405–409.
9. Arendt, R. H., Liquid-phase sintering of magnetically isotropic and anisotropic compacts of $BaFe_{12}O_{19}$ and $SrFe_{12}O_{19}$. *J. Appl. Phys.*, 1973, **44**, 3300–3305.
10. van den Broek, C. A. M. and Struits, A. L., *Ferroxdure, 37*. Philips Techn., Rundschau, 1977/1978, **37**, pp. 169–188.
11. Haberey, F., Glasbildung durch SiO_2-Zusatz bei der Herstellung von Ba- und Sr-Hexaferriten. *Ber. Dt. Keram. Ges.*, 1978, **55**, 297–301.
12. Kools, F., Effect of silica during sintering of M-type ferrites. *Ber. Dt. Keram. Ges.*, 1978, **55**, 301–304.
13. Kools, F., Reaction induced grain growth impediment during sintering of Strontium Hexaferrite with silica addition. *Solid State Ionics*, 1985, **16**, 251–260.
14. Kools, F., The action of a silica additive during sintering of strontium hexaferrite. *Sci. Sint.*, 1985, **17**, 49–80.
15. Kaneko, Y., Kitajima, K. and Takusagawa, N., Effects of CaO and SiO_2 addition on the microstructure and intrinsic coercivity of sintered Sr-Ferrite. *J. Ceram. Soc. Jpn. Intl. Ed.*, 1992, **100**, 1413–1417.
16. Chien, Y. T. and Ko, Y. C., The effect of silica characterization on the microstructure of $BaFe_{12}O_{19}$ ferrites. *J. Mater. Sci.*, 1990, **25**, 1711–1714.
17. Lee, J. W., Cho, Y. S. and Amarakoon, V. R. W., Improved magnetic properties and growth anisotropy of chemically modified Sr ferrites. *J. Appl. Phys.*, 1999, **85**, 5696–5698.
18. Besenicar, S. and Drofenik, M., High coercivity Sr hexaferrites. *J. Magn. Magn. Mater.*, 1991, **101**, 307–309.

19. Jander, W. and Hoffmann, E., Die Reaktionen zwischen Calciumoxyd und Siliziumdioxyd. *Z. Anorg. Allg. Chem.*, 1934, **210**, 211–223.
20. Philips, B. and Muan, A., Phase equilibrium diagram of the system Cao–SiO$_2$. *J. Am. Ceram. Soc.*, 1959, **42**, 414–420.
21. Goto, Y. and Takahashi, K., Phase diagram of the SrO–Fe$_2$O$_3$ system in its Fe$_2$O$_3$ rich region and the growth of SrOFe$_2$O$_3$ single crystals in composition deviated melts. *J. Jpn. Soc. Powder Metall.*, 1971, **17**, 193–197.
22. Batti, P., Diagrammi di stato, struttura e comportamento magnetico dei ferriti esagonali. *Ceramurgia*, 1976, **6**, 11–16.
23. O'Handley, R. C., *Modern Magnetic Materials*. John Wiley & Sons, New York, 2000 (p. 488).